ARTICLES
PUBLISHED ONLINE: 27 JUNE 2010 | DOI: 10.1038/NNANO.2010.115
nature nanotechnology

'Soft' Au, Pt and Cu contacts for molecular junctions through surface-diffusion-mediated deposition

Andrew P. Bonifas[1,2] and Richard L. McCreery[2,3]*

Virtually all types of molecular electronic devices depend on electronically addressing a molecule or molecular layer through the formation of a metallic contact. The introduction of molecular devices into integrated circuits will probably depend on the formation of contacts using a vapour deposition technique, but this approach frequently results in the metal atoms penetrating or damaging the molecular layer. Here, we report a method of forming 'soft' metallic contacts on molecular layers through surface-diffusion-mediated deposition, in which the metal atoms are deposited remotely and then diffuse onto the molecular layer, thus eliminating the problems of penetration and damage. Molecular junctions fabricated by this method exhibit excellent yield (typically >90%) and reproducibility, and allow examination of the effects of molecular-layer structure, thickness and contact work function.

Molecular electronics is the study of charge transport through single molecules or molecular ensembles. The term 'molecular junction' is used to describe a single molecule or a molecular ensemble oriented in parallel between conducting contacts, and is the basic component of molecular electronics. Charge transport through molecules has been investigated with techniques such as scanning tunnelling microscopy, conducting probe atomic force microscopy (AFM) and vapour deposition of top contacts[1–3]. Current–voltage measurements on molecular junctions have exhibited phenomena such as rectification and conductance switching[4–7]. The introduction of molecular electronic components into integrated circuits is the primary goal of the field.

Numerous approaches have been used to fabricate molecular layers on conducting surfaces, including self-assembly, Langmuir–Blodgett techniques, and the formation of C–C or Si–C irreversible bonds (3.5–4.0 eV) between the substrate and molecular layer[8–11]. Irreversible bonding provides the molecular layer with structural stability during subsequent fabrication and characterization processes, thus reducing the likelihood of molecular damage or metal penetration[12]. Although the resulting layers are less ordered than self-assembled monolayers (SAMs), irreversible bonding allows the formation of molecular multilayer structures in which the thickness can be controlled by altering the deposition conditions[11,13]. Our approach takes advantage of the inherent stability of the C–C bond to understand how the molecular structure and electronic coupling between the molecules and substrate influence charge transport through molecular junctions.

Although significant progress has been made in the field, the ability to fabricate robust junctions with high yields has proven experimentally difficult, primarily due to problems associated with the formation of the second contact[11]. Contact formation through vapour deposition (for example, metal evaporation) has several benefits, including the possibility of parallel fabrication, the ability to form contacts with varying work functions, and its compatibility with semiconductor processing. However, its experimental limitations include metal penetration through the molecular layer and molecular damage, resulting in behaviour characteristic of electronic shorts.

By using spectroscopic techniques, several groups have shown that direct evaporation of reactive metals such as Ti results in significant structural damage to the molecular layer[14,15]. Direct evaporation of noble metals commonly results in partial molecular damage, molecular displacement at the substrate/molecule interface, or Au penetration between the molecules[16,17]. These results depend strongly on the substrate/molecule bonding characteristics, the type of molecular layer and terminal groups. Fabrication techniques have been developed to mitigate metal penetration and molecular damage, including spin-coating of the conducting polymer contact, indirect evaporation, and the evaporation of Cu[1,7,18,19].

We report a novel technique for the formation of metallic contacts through surface-diffusion-mediated deposition (SDMD). Contact formation is achieved by direct electron-beam evaporation of a metal (Au, Cu, Pt) onto a SiO_2 surface adjacent to and ~50 nm away from the molecular layer. A SiO_2 'overhang' fabricated above the molecular layer protects the molecules from direct impingement of metal atoms and source radiation. Surface diffusion of the metal adatoms on the SiO_2 surface allows adatom migration onto the molecular layer to form the second contact. This indirect approach allows for the formation of robust Au, Cu and Pt contacts on 1–5-nm-thick molecular layers with a yield >90%.

Fabrication of molecular junctions

The SDMD fabrication process is shown schematically in Fig. 1 (for details see Supplementary Information). In brief, pyrolysed photoresist films (PPF) were fabricated on silicon substrates with a 300-nm-thick thermal SiO_2 insulating layer[20]. The PPF layer is structurally similar to glassy carbon, and provides the necessary surface chemistry to allow the formation of a C–C bond between the conducting PPF substrate and the molecular layer. A patterned etch mask was fabricated on top of the PPF surface using optical lithography, evaporation of Cr (3 nm) and SiO_2 (27 nm), and lift-off in acetone. An O_2 reactive ion etch process was used to

[1]Department of Materials, Science and Engineering, The Ohio State University, 2041 College Road, Columbus, Ohio, 43210, USA, [2]National Institute for Nanotechnology, National Research Council of Canada, Edmonton, Alberta T6G 2G2, Canada, [3]Department of Chemistry, University of Alberta, Edmonton, Alberta T6G 2R3, Canada. *e-mail: richard.mccreery@ualberta.ca

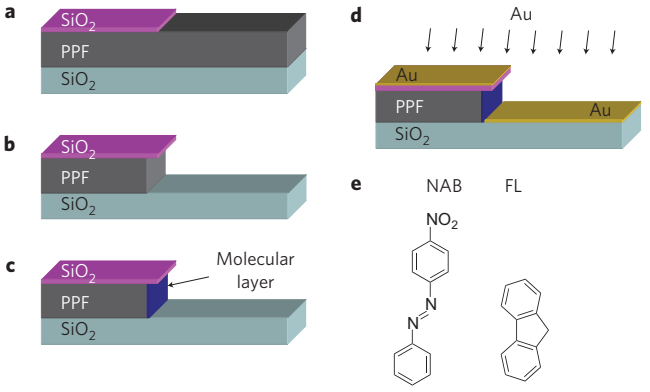

Figure 1 | Schematic of the SDMD process. a, SiO_2 etch mask patterned on a PPF layer using optical lithography. **b**, Sidewall formation using an O_2 reactive ion etch. **c**, Molecular layer formation. **d**, Au surface diffusion during metal deposition mediates second contact formation. **e**, Chemical structures of nitroazobenzene (NAB) and fluorene (FL).

etch the unmasked PPF, and conditions were selected to create a near vertical sidewall with uniform undercutting beneath the etch mask. The uniform undercutting caused the Cr/SiO_2 etch mask to overhang the underlying PPF sidewall (Fig. 2).

Molecular layers of 4-nitroazobenzene (NAB) and fluorene (FL) were electrochemically grafted to the PPF sidewall through reduction of their corresponding diazonium precursor at the PPF surface, resulting in a covalently bonded molecular layer[13]. The thicknesses of the molecular layers were measured for similar deposition conditions on a flat PPF surface using an AFM 'scratching' technique because of geometric limitations of the sidewall geometry. A comparison of the measured layer thickness and the theoretical calculated molecular length revealed that the NAB layer (4.5 ± 0.7 nm) was a multilayer consisting of 3–4 monolayers and the FL layer (1.7 ± 0.2 nm) 1–2 monolayers. As has been shown by several different laboratories, the multilayer consists of covalently bonded and conjugated subunits, which form as a result of successive attacks on the first monolayer by electrogenerated radicals[21–23]. Diaminoalkane monolayers of 1,8-diaminooctane (C_8), 1,10-diaminodecane (C_{10}) and 1,12-diaminododecane (C_{12}) were attached to the PPF sidewall by means of electrochemical oxidation. Oxidation of primary amines on a carbon surface has been shown to form monolayers through radical-assisted C–N attachment at the interface[24]. Indeed, the measured thickness of the C_8 layer was 1.1 ± 0.2 nm, indicating monolayer formation.

Metallic contacts were deposited by electron-beam evaporation of Cu, Au and Pt at a chamber pressure of $<2 \times 10^{-7}$ torr. For direct electron-beam evaporation on the molecular layers, metal deposition occurred in a direction normal to the molecular surface, without shielding of the molecular layer from radiation from the evaporation source. For SDMD, the deposition angle was varied between 0° and 15° relative to the surface normal. With a deposition angle between 0° and 5°, the overhang of the Cr/SiO_2 etch mask shadowed the molecular layer from direct impingement of both incident metal atoms and radiation from the evaporation source. At 5°, metal deposition occurred on the SiO_2 substrate about 30–80 nm laterally from the molecular layer bonded to the PPF sidewall. Figure 2 presents scanning electron microscope (SEM) and transmission electron microscope (TEM) cross-sectional images of a fabricated PPF/NAB/Au junction, showing the Cr/SiO_2 overhang, deposited 25 nm Au layer, and subsequent Au diffusion onto the NAB layer.

In SDMD, electronic contact with the molecular layer occurs by surface diffusion of the deposited metal adatoms towards and eventually on top of the molecular layer. Incorporation of diffusing adatoms at the edge of the deposited metal film causes the edge to migrate towards the molecular layer. Surface diffusion of adatoms is characterized by the equations

$$D_s = \lambda^2 \upsilon_s \exp\left(-\frac{\Delta G_s}{kT}\right)$$

and

$$\bar{x} = 2\sqrt{D_s t}$$

where λ is the hop distance, υ_s the hop frequency, ΔG_s is the activation energy, k is Boltzmann's constant, T is temperature, t is the diffusion time, and $\bar{x}$ is the average diffusion. With a typical Au (or Cu) surface diffusion activation energy of between 0.6 and 0.7 eV, the average diffusion length is 50–350 nm at 300 K for 500 s (the deposition time)[25,26], although surface heating caused by radiation and metal condensation can lead to additional surface diffusion. Because metal deposition occurs ~30–80 nm from the molecular layer, the typical surface diffusion of Au adatoms is sufficient to allow the contact to become incident on the molecular layer. As shown in the bright-field TEM image (Fig. 2b), the Au layer diffused about 150 nm above the SiO_2 surface.

Current densities were calculated using the measured metal diffusion distance onto the molecular layer, as observed by electron microscopy, where the diffusion length onto the molecular layer is dependent on the terminal group of the molecular layer, deposition parameters and diffusivity of the metallic contact. The diffusion length was measured using back-scattered SEM imaging of cross-sections of each type of molecular layer and metallic contact. Deposition of 25 nm of Au, Cu and Pt at an angle of 5° relative to the surface normal resulted in electronic contact with the

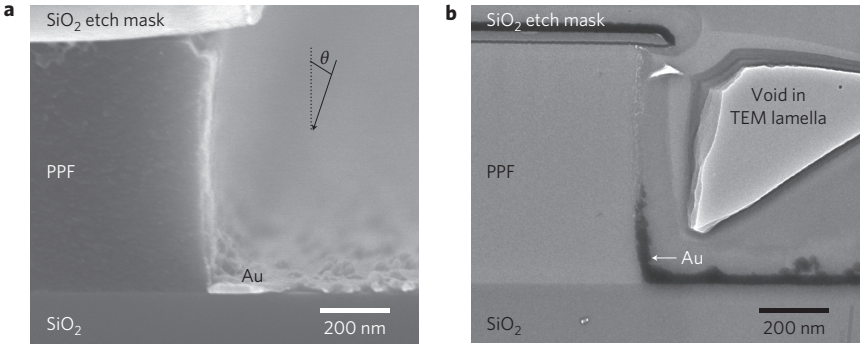

Figure 2 | Cross-section of a PPF/NAB/Au junction. a,**b**, Secondary electron SEM (**a**) and bright-field TEM (**b**) images showing the Cr/SiO_2 'overhang' after the O_2 reactive ion etch and deposition of 25 nm Au. The secondary electron SEM could not resolve the Au on the PPF sidewall because of surface charging effects. The bright region in the TEM image is caused by a void in the TEM lamella. The molecular layer is not resolved in either image.

molecular layer. In contrast, deposition of 25 nm of Cr resulted in junctions with open circuits, which was a result of a lower surface diffusivity, most probably due to surface reactions. SEM images of the Au and Cr junctions revealed that the Cr layer did not reach the molecular layer[25,27] (Supplementary Fig. S5 and Table S1).

Electronic characterization

Molecular junctions were characterized by means of current density–voltage (J–V) measurements under laboratory ambient conditions, and are shown in Figs 3– 5. For PPF/NAB/Au junctions (Fig. 3a), J–V curves for direct evaporation and SDMD show significant differences in shape and current density. Direct evaporation of Au results in a high current density and the nearly linear J–V response characteristic of an electronic short between the PPF and Au. Raman spectroscopy of the NAB layer before and after direct Au deposition shows no apparent structural changes, suggesting that the shorted junctions are caused by Au penetration (Supplementary Fig. S4). In contrast, Au junctions fabricated with SDMD exhibit a nonlinear J–V response similar to reported conductor/molecule/metal junctions made with indirect metal deposition[18]. Comparable differences between direct evaporation and SDMD are observed for junctions containing FL layers and junctions with a Pt contact.

Deposition of Cu contacts results in similar J–V responses for both deposition methods (Fig. 3b). We have previously reported that highly reproducible molecular junctions can be fabricated by direct evaporation of Cu without the presence of observable metal penetration into the molecular layer[1], yielding J–V characteristics with the same shape and magnitude as those obtained with SDMD. Although expected, the overlap in the J–V curves for direct and SDMD PPF/NAB/Cu junctions shows that two distinctly different deposition techniques result in junctions with similar electronic behaviour. Furthermore, these results show that Au and Pt penetration into the molecular layer can be minimized with SDMD.

Figure 4a,b shows J–V curves plotted on a log scale for various junctions, with the standard deviations indicated for at least five different junctions prepared simultaneously. The large decrease in current density with the incorporation of a molecular layer between the PPF and metallic contacts indicates that the current is dominated by charge transport through the molecular layer. A comparison of various molecular layers shows that the J–V characteristics depend strongly on the thickness and structure of the molecular layer.

Figure 4b compares the J–V responses for PPF/NAB with Cu, Au and Pt top contacts, a comparison that cannot be achieved through direct evaporation alone due to Au and Pt penetration. The observed trend in current asymmetry (J_{pos}/J_{neg}) is consistent with charge transport through the highest occupied molecular orbital (HOMO), as has been suggested by several groups[28–30]. As the work function of a contact increases, the barrier between the HOMO and the Fermi energy of the contact decreases, allowing more efficient transport thought the HOMO. The work function of the PPF contact is 4.93 eV, and that of electron-beam deposited Cu is 4.73 eV, as determined with a Kelvin probe[30]. For PPF/NAB/Cu junctions, the lowest barrier for hole conduction is between the PPF and HOMO, resulting in a higher current when the PPF is biased positively. For PPF/NAB/Pt junctions, the lowest barrier is between the HOMO and Pt, resulting in a higher current when the PPF is biased negatively (Pt biased positively). Although the above model is consistent with the observed asymmetry, unequivocally determining the dominant charge carrier is complicated by the unknown nature of energy level alignment within a molecular layer.

Other considerations, although not all inclusive, that need to be taken into account are the effect of interfacial dipoles and molecular energy level broadening. Varying the work function of the second

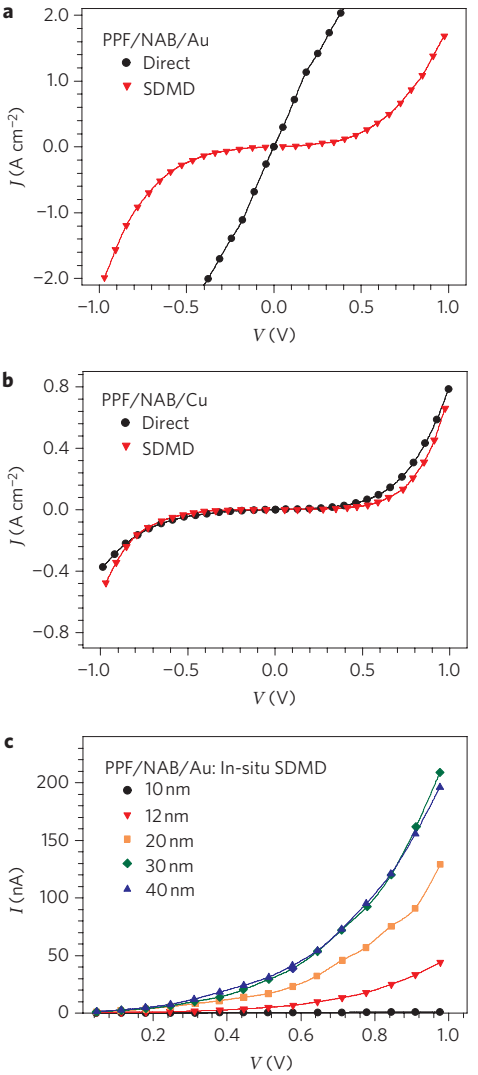

Figure 3 | J–V measurements for different deposition techniques. a,**b**, Plots of current density versus voltage for direct evaporation (black) and SDMD (red), showing large differences between the characteristics for Au-contacted junctions made with the two techniques (**a**), and similar characteristics for Cu-contacted junctions (**b**). **c**, Plots of current versus voltage measured *in situ* for Au-contacted junctions made with SDMD with five different thicknesses of Au. Current is plotted instead of current density in this figure because the contact area increases with Au thickness, until it apparently reaches a maximum area at a thickness of about 30 nm. For all measurements, positive bias indicates that the PPF is positive relative to the metal contact.

contact by ~0.7 eV (for Cu to Pt) resulted in a current–density change of less than an order of magnitude, which is similar to that observed for the contact resistance of alkanedithiols[31]. Although this small effect of work function is not expected when considering off-resonance tunnelling models, deviations from these models are expected for NAB junctions with molecular energy levels near the Fermi energy of the contacts. Most tunnelling models assume that all of the applied voltage appears across the molecular layer, neglecting the possible effects associated with a voltage drop at the contact/molecule interface. A more complete understanding of energy level alignment within a molecular layer is needed to fully understand the effect of work function on current density.

In situ current–voltage (I–V) curves were measured for an SDMD-fabricated PPF/NAB/Au junction during Au deposition by means of an electrical pass-through in the evaporation

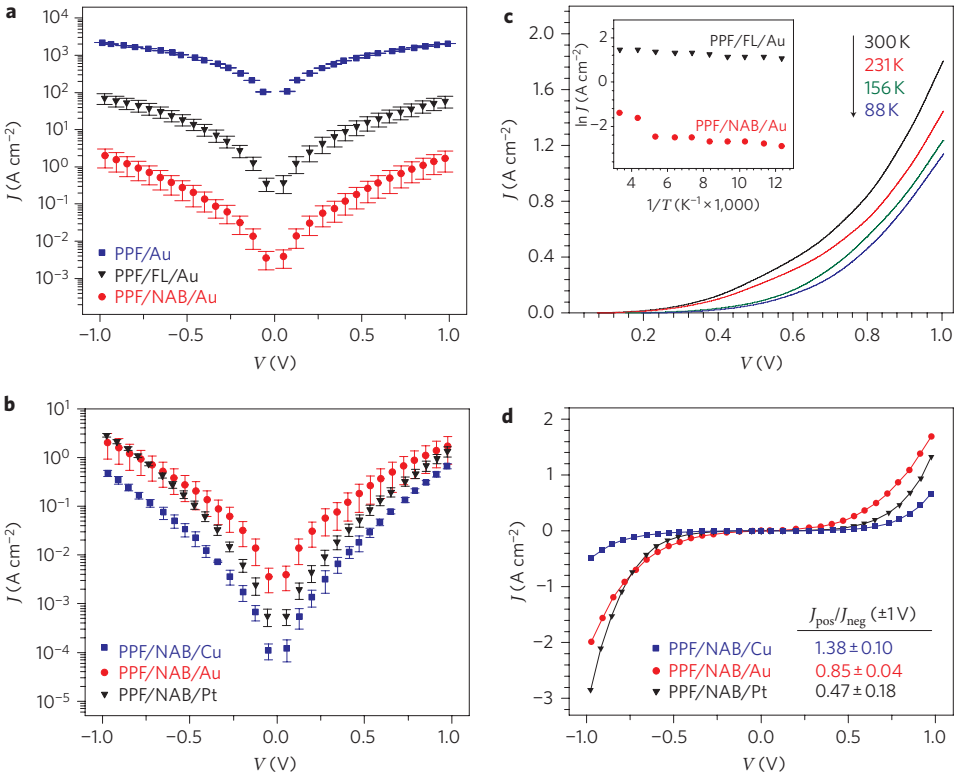

Figure 4 | *J–V* measurements for SDMD junctions with various molecular layers and top contacts. a, Plots of current density (on a logarithmic scale) versus voltage for gold contacts with (black and red) and without (blue) a molecular layer. The current density is strongly reduced by the presence of a FL (black) or NAB (red) molecular layer. **b**, Plots of current density (on a logarithmic scale) versus voltage for Cu (blue), Au (red) and Pt (black) contacts on NAB junctions resulted in similar responses, with current densities ranging over an order of magnitude. Error bars in **a** and **b** represent the standard deviation for a minimum of five junctions on one test chip. **c**, Plots of current density versus voltage for PPF/NAB/Au at four different temperatures. Inset: Arrhenius plots of the logarithm of the current density at 0.5 V versus the inverse of temperature (between 80 and 300 K) for PPF/NAB/Au (red) and PPF/FL/Au (black) junctions. The current density shows a minimal dependence on temperature in this range. **d**, The asymmetry in the *J–V* measurements becomes more obvious when the current density is plotted with a linear *y*-axis, as can be seen when the data in Fig. 4b are replotted. Inset: the measured asymmetry ratio at ±1 V.

chamber. As shown in Fig. 3c, the onset of current occurred between Au depositions of 10 and 12 nm (mass thickness). The invariant shape of the *I–V* measurements with Au deposition indicates consistent contact formation at the NAB/Au interface (Supplementary Fig. S7). With 30 nm of deposited Au, the increase in current levels off, indicating the junction is approaching a constant contact area. *In situ* current measurements during gradual SDMD should allow the stepwise formation of molecular junctions from the initial contact of a single molecule to a larger area comprising an ensemble of molecules.

Low-temperature *J–V* curves for SDMD junctions were measured in a cryogenic probe station evacuated to 5×10^{-6} torr (Fig. 4c). For the temperature range 81–188 K, the measured activation energies for the NAB/Au and FL/Au junctions were <0.003 eV, substantially less than expected for activated charge transport mechanisms such as redox exchange or molecular conformation changes. The small activation barrier may originate outside the junction, because correction of lead or contact resistance of the metal contact cannot readily be achieved with SDMD junctions.

The *J–V* characteristics of PPF/diaminoalkane/Au junctions fabricated by SDMD are shown in Fig. 5. Direct Au evaporation on diaminoalkane monolayers resulted in electronic shorts, demonstrating the 'soft' nature of the SDMD technique (inset). For C_8, C_{10} and C_{12} junctions, charge transport is consistent with off-resonance tunnelling, where the current density decreases exponentially with molecular length (N) according to $J \propto \exp(-\beta N)$. The observed decay constant β was 1.1 per carbon atom (0.88 Å^{-1}), in agreement with the literature[31,32], providing strong evidence that the measured current propagates through the molecular layer and is not associated with transport through pin holes or metal filaments. The current densities of FL (1.7 ± 0.2 nm) and C_{12} (1.6 ± 0.2 nm) junctions differ by two orders of magnitude, indicating that conjugation within the molecular layer strongly affects charge transport. Compared to C_{12}, the conjugated FL layer has molecular energy levels closer to the Fermi energy of the contacts, resulting in higher conductance.

Surface diffusion mechanism

Thin-film deposition processes can be separated into two phases: the accommodation and diffusion periods. During the accommodation period, kinetic energy perpendicular to the surface is transferred into the parallel direction and surface heat within a few atomic jump distances[33]. After the accommodation period, the adatoms are in equilibrium with the film surface and undergo surface diffusion. Surface diffusion continues until the metal adatom is trapped by chemisorption (for example, surface kink, reactive functional group) or is buried by newly arriving metal atoms.

For direct evaporation, penetration of metal atoms into the molecular layer can occur during both the accommodation and diffusion periods on the molecular layer. The degree of penetration presumably depends on the kinetic energy of the incident metal atoms, chemical interactions and heat of condensation. Previous reports have shown that a reduction in the kinetic energy of incident

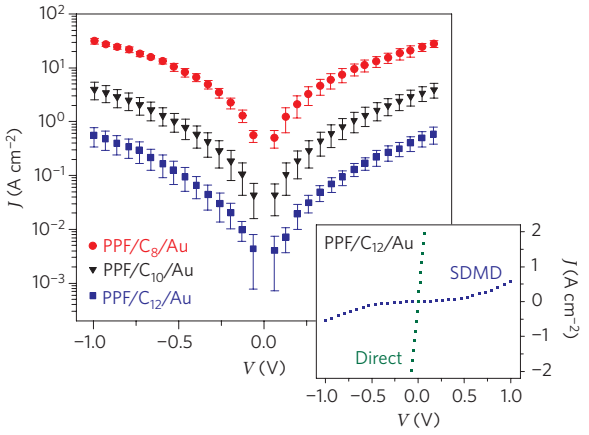

Figure 5 | *J–V* measurements for diaminoalkane monolayer junctions. Plots of current density (on a logarithmic scale) versus voltage for C_8 (red), C_{10} (black) and C_{12} (blue) junctions with Au top contacts made using the SDMD technique. Error bars represent the standard deviation for a minimum of five junctions on one test chip. Inset: plots of current density (on a linear scale) versus voltage for PPF/C_{12}/Au junctions made using direct (green) and SDMD (blue) evaporation.

Au atoms decreases the tendency for metal penetration into a molecular layer[7,18]. Direct evaporation of Cu on chemisorbed molecular layers has been demonstrated without observable penetration, in contrast to the case for Au contacts[1,34]. The high tendency for Au penetration when compared to Cu could be due to differences in surface energy, reactivity with surface functional groups[35] or the lower heat of vaporization of Cu. The higher oxidation affinity of Cu compared to Au or Pt could result in Cu oxidation during deposition, thus reducing the tendency for Cu penetration, although previous X-ray photoelectron spectroscopy depth profiling showed no detectable oxygen at the carbon/Cu interface in PPF/Cu devices[1]. The fact that the SDMD technique results in non-shorted junctions for Cu, Au and Pt implies a fundamentally different deposition mechanism from direct evaporation.

For SDMD, direct impingement of metal atoms on the molecular layer is prohibited by the overhanging SiO_2 layer. As a result, the accommodation period occurs off the molecular layer, thus remotely dissipating the kinetic energy and heat of condensation. Surface diffusion of the metal adatoms towards the molecular layer during the evaporation process causes the leading edge of the metal layer to migrate towards and finally become incident on the molecular layer. When a diffusing adatom arrives at the leading edge of the metal film, the adatom is coordinated by several other adatoms (three for a single layer of {111} Au). For the adatom to dissociate from the metal edge and diffuse onto the surface or into the interior of the molecular layer, the adatom must overcome the binding energy associated with its coordination. Using effective medium theory, the binding energy (E_b) of a fcc metal as a function of coordination number follows the equation

$$E_b(C) = E_c\left(\frac{C}{12}\right)^{0.3}$$

where C is the coordination number and E_c is the cohesive energy of Au (3.81 eV) or Cu (3.49 eV)[36]. For example, an Au atom coordinated with two Au atoms has a binding energy of 2.2 eV. This binding energy provides an energetic barrier that prevents a diffusing adatom from dissociating and diffusing into the molecular layer. Because the activation energy for surface diffusion is lower than the binding energy, an influx of metal adatoms by means of surface diffusion can occur at energies significantly below the binding energy. In contrast to direct evaporation, adatoms incident on the molecular layer are coordinated during the entire SDMD process, providing a constant barrier to metal penetration. Because this barrier is larger than any anticipated attraction between the molecular layer interior and the dissociated metal atom, significant penetration and filament formation is prevented.

Summary

We have introduced SDMD as a reliable method with which to fabricate metallic second contacts on covalently attached molecular layers. For the case of a Cu top contact, the SDMD current–voltage response agrees quantitatively with those from direct Cu deposition, but Au and Pt deposition was successful only with the SDMD technique. Electronic and spectroscopic characterization of junctions fabricated with direct Au or Pt evaporation is consistent with filament formation caused by metal penetration. In contrast, the SDMD technique prevents observable metal penetration, resulting in robust molecular junctions with all three metals. We have proposed that penetration of incident metal atoms can be prevented by ensuring the presence of metal–metal bonds at the molecule/metal interface. For SDMD, the influx of adatoms is controlled through surface diffusion, ensuring continuous metal–metal binding as the metallic contact forms on the molecular layer. The ability to vary the work function of the second contact provides a crucial experimental tool, allowing insight behind charge transport in molecular junctions. In addition, *in situ* monitoring of the SDMD process should allow characterization of the stepwise junction progression from single/several molecules to many molecules. The SDMD technique should be applicable to a wide range of additional molecular and organic systems.

Received 12 February 2010; accepted 13 May 2010; published online 27 June 2010

References

1. Bergren, A. J., Harris, K. D., Deng, F. J. & McCreery, R. L. Molecular electronics using diazonium-derived adlayers on carbon with Cu top contacts: critical analysis of metal oxides and filaments. *J. Phys. Condens. Matter* **20,** 374117 (2008).
2. Choi, S. H., Kim, B. & Frisbie, C. D. Electrical resistance of long conjugated molecular wires. *Science* **320,** 1482–1486 (2008).
3. Xu, B. & Tao, N. J. Measurement of single-molecule resistance by repeated formation of molecular junctions. *Science* **301,** 1221–1223 (2003).
4. Blum, A. S. *et al.* Molecularly inherent voltage-controlled conductance switching. *Nature Mater.* **4,** 167–172 (2005).
5. Chabinyc, M. L. *et al.* Molecular rectification in a metal–insulator–metal junction based on self-assembled monolayers. *J. Am. Chem. Soc.* **124,** 11730–11736 (2002).
6. Scott, A., Janes, D. B., Risko, C. & Ratner, M. A. Fabrication and characterization of metal–molecule–silicon devices. *Appl. Phys. Lett.* **91,** 033508 (2007).
7. Metzger, R. M., Xu, T. & Peterson, I. R. Electrical rectification by a monolayer of hexadecylquinolinium tricyanoquinodimethanide measured between macroscopic gold electrodes. *J. Phys. Chem. B* **105,** 7280–7290 (2001).
8. Wang, W. *et al.* Probing molecules in integrated silicon–molecule–metal junctions by inelastic tunneling spectroscopy. *Nano Lett.* **8,** 478–484 (2008).
9. Richter, C. A., Stewart, D. R., Ohlberg, D. A. A. & Williams, R. S. Electrical characterization of Al/AlO_x/molecule/Ti/Al devices. *Appl. Phys. A* **80,** 1355–1362 (2005).
10. Love, J. C., Estroff, L. A., Kriebel, J. K., Nuzzo, R. G. & Whitesides, G. M. Self-assembled monolayers of thiolates on metals as a form of nanotechnology. *Chem. Rev.* **105,** 1103–1169 (2005).
11. McCreery, R. L. & Bergren, A. J. Progress with molecular electronic junctions: meeting experimental challenges in design and fabrication. *Adv. Mater.* **21,** 4303–4322 (2009).
12. Walker, A. V. *et al.* The dynamics of noble metal atom penetration through methoxy-terminated alkanethiolate monolayers. *J. Am. Chem. Soc.* **126,** 3954–3963 (2004).
13. Anariba, F., DuVall, S. H. & McCreery, R. L. Mono- and multilayer formation by diazonium reduction on carbon surfaces monitored with atomic force microscopy 'scratching'. *Anal. Chem.* **75,** 3837–3844 (2003).
14. Richter, C. A., Hacker, C. A. & Richter, L. J. Electrical and spectroscopic characterization of metal/monolayer/Si devices. *J. Phys. Chem. B* **109,** 21836–21841 (2005).

15. Walker, A. V. *et al.* Chemical pathways in the interactions of reactive metal atoms with organic surfaces: vapor deposition of Ca and Ti on a methoxy-terminated alkanethiolate monolayer on Au. *J. Phys. Chem. B* **109,** 11263–11272 (2005).
16. Haick, H. & Cahen, D. Making contact: connecting molecules electrically to the macroscopic world. *Prog. Surf. Sci.* **83,** 217–261 (2008).
17. Zhu, Z. H. *et al.* Controlling gold atom penetration through alkanethiolate self-assembled monolayers on Au {111} by adjusting terminal group intermolecular interactions. *J. Am. Chem. Soc.* **128,** 13710–13719 (2006).
18. Haick, H., Ambrico, M., Ghabboun, J., Ligonzo, T. & Cahen, D. Contacting organic molecules by metal evaporation. *Phys. Chem. Chem. Phys.* **6,** 4538–4541 (2004).
19. Van Hal, P. A. *et al.* Upscaling, integration and electrical characterization of molecular junctions. *Nature Nanotech.* **3,** 749–754 (2008).
20. Ranganathan, S. & McCreery, R. L. Electroanalytical performance of carbon films with near-atomic flatness. *Anal. Chem.* **73,** 893–900 (2001).
21. Brooksby, P. A. & Downard, A. J. Electrochemical and atomic force microscopy study of carbon surface modification via diazonium reduction in aqueous and acetonitrile solutions. *Langmuir* **20,** 5038–5045 (2004).
22. Pinson, J. & Podvorica, F. Attachment of organic layers to conductive or semiconductive surfaces by reduction of diazonium salts. *Chem. Soc. Rev.* **34,** 429–439 (2005).
23. Kariuki, J. K. & McDermott, M. T. Formation of multilayers on glassy carbon electrodes via the reduction of diazonium salts. *Langmuir* **17,** 5947–5951 (2001).
24. Deinhammer, R. S., Ho, M., Anderegg, J. W. & Porter, M. D. Electrochemical oxidation of amine-containing compounds—a route to the surface modification of glassy-carbon electrodes. *Langmuir* **10,** 1306–1313 (1994).
25. Liu, C. L., Cohen, J. M., Adams, J. B. & Voter, A. F. EAM study of surface self-diffusion of single adatoms of FCC metals Ni, Cu, Al, Ag, Au, Pd and Pt. *Surf. Sci.* **253,** 334–344 (1991).
26. Speller, S., Molitor, S., Rothig, C., Bomermann, J. & Heiland, W. Surface mobility on the Au(110) surface observed with scanning tunneling microscopy. *Surf. Sci.* **312,** L748–L752 (1994).
27. Racz, Z. & Seabaugh, A. Characterization and control of unconfined lateral diffusion under stencil masks. *J. Vac. Sci. Technol. B* **25,** 857–861 (2007).
28. Reddy, P., Jang, S. Y., Segalman, R. A. & Majumdar, A. Thermoelectricity in molecular junctions. *Science* **315,** 1568–1571 (2007).
29. Beebe, J. M., Kim, B., Frisbie, C. D. & Kushmerick, J. G. Measuring relative barrier heights in molecular electronic junctions with transition voltage spectroscopy. *ACS Nano* **2,** 827–832 (2008).
30. Yan, H. J. & McCreery, R. L. Anomalous tunneling in carbon/alkane/TiO_2/gold molecular electronic junctions: energy level alignment at the metal/semiconductor interface. *ACS Appl. Mater. Interfaces* **1,** 443–451 (2009).
31. Engelkes, V. B., Beebe, J. M. & Frisbie, C. D. Length-dependent transport in molecular junctions based on SAMs of alkanethiols and alkanedithiols: effect of metal work function and applied bias on tunneling efficiency and contact resistance. *J. Am. Chem. Soc.* **126,** 14287–14296 (2004).
32. Holmlin, R. E. *et al.* Electron transport through thin organic films in metal–insulator–metal junctions based on self-assembled monolayers. *J. Am. Chem. Soc.* **123,** 5075–5085 (2001).
33. Abelmann, L. & Lodder, C. Oblique evaporation and surface diffusion. *Thin Solid Films* **305,** 1–21 (1997).
34. Anariba, F. *et al.* Comprehensive characterization of hybrid junctions comprised of a porphyrin monolayer sandwiched between a coinage metal overlayer and a Si(100) substrate. *J. Phys. Chem. C* **112,** 9474–9485 (2008).
35. Nowak, A. M. & McCreery, R. L. Characterization of carbon/nitroazobenzene/titanium molecular electronic junctions with photoelectron and Raman spectroscopy. *Anal. Chem.* **76,** 1089–1097 (2004).
36. Ibach, H. *Physics of Surfaces and Interfaces* (Springer, 2006).

Acknowledgements

The authors acknowledge financial support from the National Sciences and Research Council of Canada, the Alberta Ingenuity Fund, the University of Alberta, and the National Institute for Nanotechnology (NINT). We acknowledge P. Li for FIB-TEM analysis, K. Harris and H. Yan for scientific discussions, and B. Szeto for technical assistance.

Author contributions

A.B. and R.M. conceived and designed the experiments, A.B. performed the experiments, A.B. and R.M. co-wrote the manuscript and Supplementary Information.

Additional information

The authors declare no competing financial interests. Supplementary information accompanies this paper at www.nature.com/naturenanotechnology. Reprints and permission information is available online at http://npg.nature.com/reprintsandpermissions/. Correspondence and requests for materials should be addressed to R.L.M.